Nuclear magnetic resonance in single crystals of dilute magnetic alloys

Thomas S. Stakelon* and Charles P. Slichter
Department of Physics, Materials Research Laboratory, University of Illinois at Urbana-Champaign, Urbana, Illinois 61801
(Received 28 April 1976)

We have observed nuclear resonances from ^{63}Cu nuclei in the first few shells around Fe, Co, and Ni impurities present in low concentrations of single crystals of copper. The resonances appear as weak satellites displaced in field δH form the much stronger resonance from ^{63}Cu nuclei far from the impurities. Study of the dependence of the various δH's on the orientation of the static field $\vec{H}_0$, with respect to the crystal axes enables one to determine which satellites go with which shell of neighbors, and to deduce the quadrupolar, dipolar, and pseudodipolar coupling parameters for the observed shells. By these means we have been able to assign shells to satellites seen in powder samples. For *Cu*Fe we identify the second and third shells, for *Cu*Co the first and second, and for *Cu*Ni the first. The observation that the pseudodipolar coupling of the first shell in *Cu*Co is strongly nonaxial proves that there are strong crystal-field effects. For the first neighbor to the Co the pseudodipolar coupling is about twice the direct dipolar coupling. For *Cu*Fe the same is true for the third neighbor shell.

I. INTRODUCTION

Properties of dilute alloys of magnetic atoms in nonmagnetic host metals have generated intense experimental and theoretical interest during the past 15 years.[1-5] The classic series of such alloys is the 3-*d* row of transition elements (Sc, Ti, V, Cr, Mn, Fe, Co, Ni) dissolved in the noble metals. Our group has studied all eight atoms dissolved in Cu. In this paper we report nuclear-magnetic-resonance studies of single crystals of copper containing iron, cobalt, or nickel, aimed at measuring the magnetization density at Cu nuclei in the vicinity of the magnetic atom. The use of single crystals has yielded new information, including positive identification of the crystallographic location of the nuclei under observation with respect to the magnetic-impurity atom, as well as the electric quadrupole, magnetic dipolar, and pseudodipolar couplings of the near neighbors. The results demonstrate for the first time the role of the crystal field acting on iron-group atoms in a noble metal.

Numerous NMR studies have been made of Cu containing iron-group atoms. These include studies of host metal NMR associated with Cu atoms far from the impurity — the so-called main line, NMR of the impurity itself, and NMR of nuclei which are near neighbors of the magnetic atom. The near neighbors show up as weak resonances which are satellites of the main line. All these sorts of experiments are usually carried out on powder samples to permit penetration of the alternating fields associate with the NMR.

Single-crystal studies of impurities were first performed by Schumacher and Schnakenberg.[6,7] They observed the satellites from Cu nuclei which were in the first or second shell of neighbors to nonmagnetic impurities. They were able to identify the shell because the lines were displaced by the electric quadrupole coupling whose effect depended on the orientation of the static magnetic field H_0 with respect to the principal axes of the electric field gradient, and the orientation of those principal axes with respect to the crystal axes. Jensen, Nevald, and Williams did similar studies.[8]

In this paper we report the first single-crystal studies of magnetic atoms in noble metals. We report our results on dilute alloys of Cu containing 800–7000 ppm of Fe, Co, or Ni.

These data yielded positive identification of satellite resonances from the following neighboring shells of nuclei around the 3*d* transition-element impurity: *Cu*Fe, second and third; *Cu*Co, first and second; *Cu*Ni, first. Large anisotropic field shifts due to the magnetic hyperfine interaction were measured at copper nuclei in the third-shell neighboring Fe atoms and the first-shell neighboring Co atoms in their respective alloy single crystals. The size and asymmetry of the interaction indicates a large pseudodipolar contribution to the magnetic hyperfine field. The electric-field-gradient tensor was determined at nuclei in the first-neighbor shells around the magnetic atoms in *Cu*Co and *Cu*Ni. The isotropic field shifts due to the contact term of the magnetic hyperfine interaction was measured for satellites from the above and other shells of neighboring copper nuclei.

The usual treatment of magnetic atoms in nonmagnetic hosts is the Friedel-Anderson[9] theory. In that theory, the strength of the magnetic moment is determined by the extent to which the Coulomb interaction, which repels the transition-element *d*-orbital electrons of opposite spin, can overcome *d*-orbital mixing with the weakly correlated host

conduction electrons. The resultant picture of a magnetic atom is two scattering resonances, one for up spins, the other for down spins, displaced in energy with respect to one another. The associated scattering phase shifts give rise to a spatial oscillation of the conduction-electron spin polarization in the vicinity of the magnetic atom, hence to shifts of the NMR of the Cu nuclei in the vicinity of the magnetic atom. Measurement of those shifts in principle permits one to determine the energies and widths of the scattering resonances, provided one can identify the crystallographic position of the nucleus giving rise to the resonance. That identification is a major objective of our work. Boyce and Slichter have used our results to determine the scattering resonances of Fe in Cu.

An interesting result of our measurements is proof, from the symmetry of the pseudodipolar coupling of the nearest-neighbor Cu atoms to the Co in *Cu*Co that the crystal electric fields are significant.

In Sec. II we give the theory of single-crystal spectra. Section III presents the experimental details. The results are given in Sec. IV. Section V presents the conclusions.

II. SINGLE-CRYSTAL SATELLITE SPECTRA

A. General aspects

We turn now to the nuclear interactions responsible for the anisotropic satellite resonance shifts seen in NMR experiments on dilute alloys in the form of single crystals. The shifts are caused by the hyperfine and the quadrupole interactions.

The hyperfine coupling arises from the interaction of a nuclear moment with the magnetic field produced by the spin and orbital motion of nearby electrons.[10] In general, this magnetic field is due to the electron magnetization at the nuclear site, known as the contact term, plus a contribution of dipolar form due to electrons at a distance. In a pure copper crystal in a static magnetic field, the contact term is nonzero due to the slight paramagnetism of the conduction electrons. The dipolar and quadrupolar contributions vanish, however, due to the cubic symmetric of the lattice. When a magnetic impurity is introduced, the hyperfine and quadrupolar interactions at nearby nuclei are changed, the change roughly falling off with distance from the magnetic atom. Not only is the contact term different for distinct shells of nuclei around the impurity, but the dipolar and quadrupolar contributions are nonzero due to the lowered symmetry near the impurity. In a resonance experiment at fixed frequency the contact term causes resonance field shifts of nearby nuclei which are independent of the orientation of the applied magnetic field with respect to the crystal axes for our case of an isotropic susceptibility of the magnetic atom. But the existence of the dipolar terms cause the shift of the resonances of neighboring nuclei to depend upon the orientation of the applied field with respect to the crystal axes. Whether or not one can observe these effects depends on whether or not (i) the satellite is shifted enough to be out from under the main line, and (ii) whether or not the anisotropic splittings are large enough compared to the width of the satellite resonance to give a resolved structure which changes with magnetic field direction.

B. Hyperfine coupling

The energy of interaction $E_{n\sigma}$ between a nucleus and a nearby electron in a state with orbital and spin quantum numbers n and σ, respectively, can be written[10]

$$E_{n\sigma} = \gamma_e \gamma_N \hbar^2 \vec{I} \cdot \langle n, \sigma | \tfrac{8}{3}\pi \vec{s}\delta(\vec{r}) + [3\vec{r}(\vec{r}\cdot\vec{s}) - r^2\vec{s}]/r^5 + \vec{l}/r^3 | n, \sigma \rangle, \quad (1)$$

where γ_e is the electron gyromagnetic ration, $\vec{s}$ and $\vec{l}$ are the electron-spin and orbital angular momentum operators, respectively, and $\vec{r}$ is the position of the electron relative to the nucleus. The first term is called the contact term and the second arises from the dipolar interaction between the electron and nuclear spins. The third term gives the interaction of the nucleus with the magnetic field produced by the electron orbital motion. The total hyperfine interaction must include the contribution from all occupied electron states.

In a pure-metal single crystal, the contact term results in an additional effective field $\Delta\vec{H}$, which is the same at every nucleus and parallel to the applied field $\vec{H}_0$. The quantity $\Delta H/H_0$, denoted by K, is the Knight shift which, for ^{63}Cu nuclei in copper metal, is equal to 0.002 32. The remaining terms in Eq. (1) vanish in first approximation in a pure copper crystal due to the cubic symmetry of the lattice, though in a higher approximation the last term when combined with the Zeeman coupling of the electron orbital magnetic moment gives rise to a chemical shift[10] since the applied static field induces a net orbital moment. Walstedt and Yafet[10b] have argued that the chemical shift may contribute about $\frac{1}{4}$ of the observed Knight shift of pure copper. If they are correct, it should also contribute to the satellite splittings to the extent that the presence of the magnetic atom changes this term at a neighbor relative to the pure host.

Near a magnetic impurity in an alloy single crystal, the spin magnetization density will be nonuniform. As a result, for each distinct shell of

nuclei around the impurity, the contact term will give a field shift which differs from that of the pure metal by

$$\delta H = \tfrac{8}{3}\pi \delta m_s(0), \tag{2}$$

where $\delta m_s(0)$ is the change in the spin magnetization density at the nuclear site due to the magnetic impurity. Since the copper lattice is cubic, the impurity susceptibility will be isotropic and the magnitude of the spin magnetization density at the nuclear site will be independent of the applied field orientation. It is convenient to define the following field-independent quantity associated with each distinct shell of nuclei around the magnetic impurity:

$$\Delta K/K \equiv \delta H/\Delta H = \delta m_s(0)/m_s(0). \tag{3}$$

Owing to the lowered symmetry around nuclei near a magnetic impurity, the last two terms in Eq. (1) will contribute a magnetic field at the nucleus. Since the resulting resonance field shift is anisotropic, the contribution to the nuclear spin Hamiltonian arising from the hyperfine interaction $\mathcal{H}_{\rm hf}$ is properly written in terms of a tensor[10] (the Knight-shift tensor) $\vec{\vec{K}}$:

$$\mathcal{H}_{\rm hf} = -\gamma_N \hbar \vec{I} \cdot \vec{\vec{K}} \cdot \vec{H}_0. \tag{4}$$

Only that component of the vector $\vec{\vec{K}} \cdot \vec{H}_0$ parallel to the applied field $\vec{H}_0$ is effective in shifting the resonance. If the tensor is written in a coordinate system referred to a set of principal axes, so that it is diagonal, the effective field in the direction of the applied field will take the form

$$\delta H = -H_0 \tfrac{1}{2} K_{zz}[(3\cos^2\theta - 1) + \eta_K \sin^2\theta \cos 2\phi], \tag{5}$$

where θ and ϕ are the spherical coordinates of the external field vector in the principal-axes system of the Knight-shift tensor. Only the change in the total magnetization density due to the presence of the magnetic impurity, denoted by $\delta m_s(\vec{r})$, is responsible for the anisotropic Knight shifts. The relevant components of the Knight-shift tensor can be written

$$K_{zz} = \frac{1}{H_0}\int \delta m_s(\vec{r}) \frac{3\cos^2\theta - 1}{r^3} d\vec{r}, \tag{6}$$

$$\eta_K = (K_{xx} - K_{yy})/K_{zz} = \frac{1}{K_{zz} H_0}\int \delta m_s(\vec{r}) \frac{3\sin^2\theta \cos 2\phi}{r^3} d\vec{r}, \tag{7}$$

where r, θ, ϕ are referred to the principal-axes system.

If one chooses a set of principal axes in which the z axis is parallel to the radius joining the impurity and the nucleus, then the first term in Eq. (5) will have the form produced by a magnetic moment located at the impurity site and aligned along the external field. This would be the only term if the total magnetization density had spherical symmetry about the impurity and was located within the impurity unit cell. In this case, the anisotropic hyperfine field shift would have the form

$$\delta H = (\chi H_0/r_N^3)(3\cos^2\theta - 1), \tag{8}$$

where χ is the total susceptibility of the impurity and r_N is the distance from the impurity to the nucleus being observed. Another large contribution to the anisotropic Knight shift may originate in the unit cell of the nucleus under observation. This can occur due to the large weight given to this region by the factor $1/r^3$ in the integrands of Eqs. (6) and (7). Such a contribution to the anisotropic Knight shift is termed a pseudodipolar coupling with the magnetic impurity.

C. Electric quadrupole coupling

The nuclear quadrupole coupling arises from the interaction of the nucleus with nearby charges. In a pure copper crystal, the coupling vanishes due to the cubic lattice symmetry. When an impurity is introduced into the lattice, the coupling no longer vanishes, since the electronic charge density is changed and the nuclear charges of nearby host atoms are displaced. The resulting quadrupole interaction shifts the resonance field of host nuclei near the impurity and can lead to observable satellite resonances.

At any point in the alloy crystal lattice, one can define the second-rank electric-field-gradient (EFG) tensor, with components

$$V_{x_i x_j} = \delta V(\vec{r})/\delta x_i \delta x_j, \tag{9}$$

where $V(\vec{r})$ is the electric potential expressed as a function of the coordinates $(x, y, z) = (x_1, x_2, x_3)$. Of relevance here is the traceless EFG tensor at the site of a nucleus computed with the potential due only to charges external to the nucleus. In a pure copper crystal, cubic symmetry at each nuclear site insures that the EFG components vanish. Therefore, near an impurity atom in a copper alloy crystal, the EFG tensor can be computed with just the change in charge distribution $\delta q(\vec{r})$ due to the introduction of the impurity. In a principal-axes system, the elements of the diagonal EFG tensor are given by

$$V_{zz} = \int \delta q'(\vec{r}) \frac{3\cos^2\theta - 1}{r^3} d\vec{r}, \tag{10}$$

$$\eta_Q = (V_{xx} - V_{yy})/V_{zz} = \frac{1}{V_{zz}}\int \delta q'(\vec{r}) \frac{3\sin^2\theta \cos 2\phi}{r^3} d\vec{r}, \tag{11}$$

with

$$\delta q'(\vec{r}) = \delta q(\vec{r})[1+\gamma(r)], \tag{12}$$

where η_Q is called the asymmetry parameter, (r, θ, ϕ) are spherical coordinates referred to the principal axes, and in which $\delta q'(\vec{r})$ differs from $\delta q(\vec{r})$ as a result of the Sternheimer antishielding factor $\gamma(r)$. In general, $\delta q(\vec{r})$ can arise from a change in the conduction-electron distribution as well as the displacement of host nuclei around the impurity atom. The Sternheimer antishielding factor $\gamma(r)$ has been calculated for copper[11] and accounts for the enhancement of the quadrupole interaction due to the distortion of the core electron wave functions by charges external to the core radius. Within the core region, the antishielding factor is zero. Within this region also, according to Kohn and Vosko,[12] the largest contribution of the conduction electrons to the EFG occurs near an impurity in copper due to the factor $1/r^3$ in the integrand of Eqs. (10) and (11). In this paper we shall follow the convention that the principal axes are chosen in such a way that $|V_{zz}| \geq |V_{yy}| \geq |V_{xx}|$ and, as a consequence, $0 \leq \eta_Q \leq 1$.

Since the copper nucleus has a quadrupole moment, if the EFG tensor at the nucleus is nonzero, an additional term is added to the nuclear Hamiltonian which perturbs the nuclear energy levels. Only satellite resonances originating from a shift of the $(\frac{1}{2})$-$(-\frac{1}{2})$ transition of near-neighbor copper nuclei are identified in this report. For small enough electric field gradients, as encountered here, the $(\frac{1}{2})$-$(-\frac{1}{2})$ transition is shifted in energy only in second order by the quadrupole interaction. The resulting shift in the resonance field δH can be written

$$\delta H = (2\pi\nu_Q/\gamma_N)^2(1/H_0)f(\cos^2\theta, \cos 2\phi, \eta_Q), \tag{13}$$

where

$$\nu_Q = eQV_{zz}/4\pi h, \tag{14}$$

γ_N is the nuclear gyromagnetic ratio (for ^{63}Cu: $\gamma_N/2\pi = 1.1285$ kHz/G), e is the proton charge, Q is the nuclear quadrupole moment (0.157×10^{-24} cm^2), and f is a function of the asymmetry parameter and the angular coordinates θ and ϕ of the external field $\vec{H}_0$ with respect to the principal axes of the quadrupole tensor. The function f has been computed by Narita *et al.*[13] and is discussed by Schumacher and Schnakenberg.[6,7] Second-order quadrupole effects can be separated from magnetic hyperfine effects experimentally since the former is inversely proportional to H_0, the latter proportional to H_0.

D. Principal axes and identification of the shell

In general, the identification of the principal axes of either the magnetic hyperfine or EFG tensors for a specific shell of nuclei must be made using experimental results. Certain shells of nuclei around a substitutional impurity in copper have sufficiently high symmetry partially to determine these axes, however. In the first shell, for a nucleus at the (0, 1, 1) position, the X, Y, and Z axes must be chosen from among the [100], [011], and [0 – 1 1] directions. As Schumacher and Schnakenberg[6,7] have indicated the inversion symmetry of the lattice always allows the assignment of the [011] and [0 1 –1] directions to be interchanged without affecting the calculated satellite NMR spectrum. This resulting ambiguity is indicated in the results below by placing alternative assignments in parenthesis.

The magnitude of the resonance field shifts due to the interactions just described will ultimately determine the observed ^{63}Cu NMR spectrum. In order to observe the satellite resonance, its field shift must take it far enough from the intense main resonance to allow it be resolved. The observed satellite field shifts will depend on the angle between $\vec{H}_0$ and the electric field gradient or hyperfine tensor principal axes, and also on the magnitude of the tensor components. All the nuclei in a given shell around the magnetic impurity will have the same electric field gradient or hyperfine tensor except for the directions of the principal axes. Since the principal axes are related to each other by crystal symmetry operations, the resonances arising from a shell of nuclei will form a pattern characteristic of that particular shell as the external field is changed with respect to the crystallographic axes. Both the identity of the shell of nuclei giving rise to the satellites and the hyperfine tensor itself may be determined from the rotation pattern. To obtain this rotation pattern, it is convenient to orient the alloy crystal in the apparatus such that, by rotating about a single axis (the [1 – 1 0] axis), the three major symmetry directions ([001], [110], [111]) can be aligned parallel to the magnetic field. In these three directions, the spectrum of a shell of nuclei is simplified by the high symmetry, i.e., there are more nuclei with the same field shift, and consequently, the greatest intensity is observed for the satellite resonances.

III. EXPERIMENTAL DETAILS

Dilute alloys of nickel, cobalt, iron, manganese, and chromium in a copper host at between 0.7 and 0.08 at.% concentration were prepared in single-crystal form. The alloy crystals had the following properties: they were cylinders about 1 in. long and $\frac{3}{8}$ in. diameter, oriented with the [110] direction parallel to the cylinder axis, homogeneous (free of precipitates and having no more than a

10% concentration difference from end to end) and pure (having less than 100 ppm of impurities).

Using 99.999% pure starting materials, homogeneous alloy ingots were prepared as described by Lo *et al.*[14] These were then used for crystal growing. Nickel and cobalt crystals were grown in crucibles machined from high-purity graphite. To minimize reaction, iron alloy crystals were grown in tapered high-purity alumina tubes, the surfaces of which had a thin (about 0.05 cm) layer of 0.05-μm alumina powder fired onto its inner surface to prevent the crystal from sticking to the crucible. Below the alloy charge, a 2-in.-long pure-copper seed crystal was held in a close fitting graphite sleeve 0.25 in. in diameter. The crystal growing apparatus was similar to the one described by Young and Savage.[15] The alloy and one-half of the seed crystal were melted and then crystallized at either 1 or 2 in./h.

As grown alloy crystals were oriented along the [110] direction with an accuracy of about 2°. A section about 1 in. long was spark cut from the center of the crystal with the end faces oriented within 1° of [110] to serve as a reference when mounting in the NMR probe. Sections of the crystal were cut off immediately above and below the sample and analyzed by emission spectroscopy and spectrophotometry. The crystal was chemically etched, encapsulated in a quartz tube under $\frac{1}{3}$ atm of argon, annealed at 1060 °C for 7 days and rapidly quenched into water. This was found sufficient to produce resonance linewidths within 10% of those obtained in powder prepared directly from rapidly quenched ingots. After a light etching, the crystal was wrapped with 0.0005-in. Mylar to protect it from abrasion. The NMR coil of No. 36 enameled silver wire was wrapped directly over the Mylar. For frequencies below 10 MHz, coils were a single section closely wound over a length of 0.5 in. with a Q of approximately 2.5 at 8 MHZ. For use in the region near 60 MHz, they consisted of four closely wound sections each 0.13 in. long, placed side by side, and wired in parallel. The measured Q was about 6.0. The construction of the coils was determined by a study of the conditions necessary for maximum signal-to-noise ratio when using metallic single crystals for NMR. Results of this study will be published elsewhere. Once in the spectrometer, alignment of the alloy crystal axes with respect to the applied field was estimated to have an accuracy of 2 deg.

Two NMR spectrometers were used. One operated between 2 and 10 MHz using an iron-core electromagnet. The second spectrometer utilized a 60 kG, Nb-Ti superconducting solenoid (Westinghouse Corp.) in a room-temperature access Dewar (Janis). Measurements were made at frequencies of 49–68 MHz. Both spectrometers were bridge devices using radio-frequency hybrid junctions. Basic principles of the hybrid junction bridge circuit have been previously discussed. These spectrometers and their operation have been described by Lo *et al.*[14] and Lang *et al.*[16]

Field modulations of between 2 and 20 G in peak-to-peak amplitudes were used at frequencies of 150 and 700 Hz in the low- and high-field spectrometers, respectively. Sweep widths of 50–250 G were used with sweep times of 80–200 sec and a lock-in time constant of 3 sec. The rf phase was usually adjusted so that a slight amount of the dispersive phase was present when satellites were observed. This procedure could be used to flatten the tail of the resonance in the region of the satellite, as described by Lo *et al.*[14] Intensities of satellite resonances ranged from 10^{-1} to 10^{-4} of the main resonance intensity. Between 10 and 1200 sweeps were averaged using a Nicolet 1072 averager, depending upon the satellite intensity and involving total averaging times of up to two days.

IV. EXPERIMENTAL RESULTS

A. *Cu*Fe

1. General

^{63}Cu satellite resonances were studied at a field of 58 kG in two *Cu*Fe alloy single crystals of Fe concentrations 0.093 and 0.35 at.%. The NMR spectrum for field alignments along the three highest-symmetry axes indicated anisotropic field shifts were associated with most of the observed satellite resonances.

On the basis of the rotation pattern, we can identify Boyce and Slichter's satellite B ($\Delta K/K = -1.20$ in the powder spectra) as arising from the third shell of nuclei around Fe atoms and can determine the asymmetric magnetic hyperfine tensor associated with the shell. We find a large pseudodipolar contribution to the observed anisotropy. We assign another satellite (Boyce and Slichter's satellite M with $\Delta K/K = 1.85$) to the second shell of nuclei on the basis of the satellite's relative intensity. (See Fig. 1.)

The measurements were performed at a temperature of 298 K. A 3-sec lock-in time constant and a modulation field of 15 G at a frequency of 700 Hz were typically used. The ^{63}Cu main resonance in the 0.093-at.% sample had a signal-to-noise ratio of 100 to 1 under these conditions. The satellite intensities were between 10^{-2} and 8×10^{-4} of the main resonance. The long signal averaging times used to achieve the sensitivity needed to observe the satellites limited the magnetic field orientation to three high-symmetry

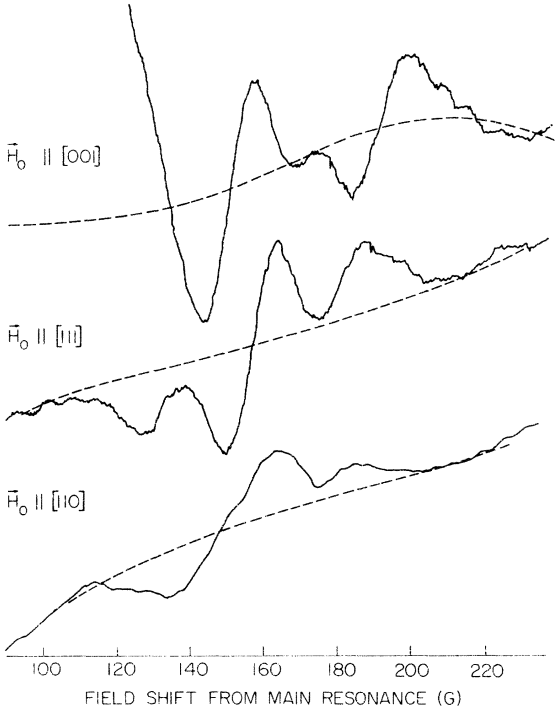

FIG. 1. Satellite spectrum in the region of satellite *B* in a single single crystal of Cu(0.093-at.% Fe). The spectrum is shown for field alignments along the three major symmetry axes. The applied magnetic field is 58 kG and the temperature is 298 K. A 3-sec lock-in time constant was used and the traces shown are the result of averaging between 300 and 800 sweeps.

directions as discussed in Sec. II. The measurements reported here were made using the 0.093-at.% sample. The same measurements were performed on the 0.35-at.% sample but, since the main resonance and satellites had twice the peak-to-peak linewidth, the resolution of the satellite spectrum was considerably poorer than in the lower concentration sample. Observations made with the 0.35-at.% sample are consistent with those reported here for the 0.093-at.% sample, however. The ^{63}Cu peak-to-peak linewidths of both samples for the three different magnetic field orientations used are listed in Table I.

Table II lists data related to satellites observed in the 0.093-at.% sample. In the study of Boyce and Slichter in powdered samples of *Cu*Fe, the strictly linear dependence of the observed satellite positions on magnetic field strength indicated their origin as due to the magnetic hyperfine interaction. The more complicated spectra obtained here with a single-crystal sample was directionally averaged in the powdered sample, resulting in fewer observed satellites — quite likely no more than one from each shell in this region of the spectrum.

TABLE I. Measured ^{63}Cu main resonance linewidths. Listed are the peak-to-peak linewidths of the ^{63}Cu main resonance of single-crystal alloy samples used in this study. The slight anisotropy observed appears due to the anisotropy of the natural linewidth due to nuclear dipole-dipole coupling in an fcc lattice. This anisotropy was observed by Sagalyn and Hofmann (Ref. 17) in a pure-copper crystal and is tabulated here as well. The impurity concentrations are in units of at.%. The linewidth is shown for magnetic field alignment along the three major symmetry axes.

Alloy crystal-field temperature	Peak-to-peak linewidth (G) [001]	[111]	[110]
Cu(0.084-at.% Co) 58 kG 293 K	8.9±0.4	10.1±0.4	9.9±0.4
Cu(0.35-at.% Co) 4.6 kG 4.2 K	6.1±0.4	7.6±0.4	7.2±0.4
Cu(0.093-at.% Fe) 58 kG 293 K	11.4±0.6	12.2±0.6	12.4±0.6
Cu(0.35-at.% Fe) 58 kG 295 K	29.6±2.0	30.6±1.3	29.9±1.3
Pure Cu	5.0±0.1	6.8±0.1	6.5±0.1

2. *Assignment of satellites*

The critical spectrum for identifying the shell of satellite *B* is that for H_0 along the [111] direction, for which there are three lines. The only shells among the ten nearest the impurity which can give rise to three distinct satellites for that orientation of the magnetic field are the third shell and the tenth shell. In view of the large field shift observed, the assignment is made to the third shell. The observed satellites have intensities in the ratio of nearly 1:2:1, as expected theoretically from the third shell. For the [001] orientation, two satellites with an intensity ratio of nearly 1 to 2 are observed in agreement with the theoretical rotation pattern of the third shell. With a [110] field orientation four lines are expected theoretically. The observed spectrum does not have that many, but the very broad absorption from 120 to 160 G is what one expect if the lines are not resolved. The four satellites that arise from the third shell with a [110] field alignment can produce the observed spectrum.

The measured field shifts of these satellites for the [001] and [111] orientations were used to find the magnetic hyperfine tensor for the third shell. The third-shell nuclei occur at (2, 1, 1) and equi-

TABLE II. Field shifts and relative intentisites of satellites in Cu(0.093-at.% Fe). Listed are the field shifts and relative intensities of satellites observed in a single crystal of CuFe 0.093 at.%. The magnetic field is applied along the three major crystal-symmetry axes. The field shifts are expressed as a fraction of the applied field divided by the Knight shifts of pure copper. Small corrections were made (≤ 0.01) to give the field shifts at 300 K. Intensities are measured relative to the intensity of the ^{63}Cu main resonance. Assignments of some of the satellites to neighboring shells of nuclei around the Fe atom and the theoretical number of nuclei corresponding to the satellite are also presented.

Field orientation	$\frac{\delta H}{H_0 K}$	10^3 fractional intensity	Shell number of nuclei
[100]	1.87 ± 0.02	2.3	2nd/6
	1.39 ± 0.08	2.5	
	0.72 ± 0.04	6.7	
	0.37 ± 0.03	2.0	
	-0.81 ± 0.04	7.7	
	-1.14 ± 0.03	2.8	3rd/16
	-1.43 ± 0.03	1.5	3rd/8
[111]	1.87 ± 0.03	2.2	2nd/6
	1.17 ± 0.02	0.81	
	0.72 ± 0.03	2.8	
	0.46 ± 0.01	3.1	
	0.29 ± 0.02	3.3	
	-0.35 ± 0.04	2.9	
	-1.03 ± 0.03	1.5	3rd/6
	-1.19 ± 0.03	3.3	3rd/12
	-1.37 ± 0.02	1.6	3rd/6
[110]	1.85 ± 0.03	1.6	2nd/6
	1.41 ± 0.03	1.0	
	0.80 ± 0.04	3.2	
	-1.15 ± 0.03	6.0	3rd[a]
	-1.34 ± 0.06	1.6	3rd[a]

[a] These satellites were poorly resolved from one another.

valent positions. They possess a plane of symmetry, which enables one to deduce one principal axis, but the other two axes can not be deduced by symmetry alone. Suppose the iron impurity is at (0, 0, 0) and a third-shell copper nucleus is at the (2, 1, 1) position. This nucleus lies in a reflection plane, the (0 1 – 1) plane, and so the [0 1 – 1] direction is a principal axis. We label it the X axis. The orientation of the Y and Z axes in the (0 1 – 1) plane can then be specified by the angle that the Z axis makes from the [100] direction by rotating in a positive sense about the X axis.

Performing the principal axis transformation, we find that the components of the magnetic hyperfine tensor are then $\Delta K/K = -1.21 \pm 0.05$, $K_{zz}/K = -0.29 \pm 0.05$, and $\eta_K = 0.30 \pm 0.06$. The direction of the Z axis is $24.9° \pm 5.6°$ from the $\langle 100 \rangle$ direction. It is noteworthy that for a copper nucleus at this position, the corresponding angle for the radial direction from the iron impurity is 35.26°. Assuming all of the spin density associated with the iron impurity is located within the impurity unit cell, one can calculate a direct dipolar contribution to the magnetic hyperfine tensor. With a radial Z principal axis, the direct dipolar tensor components are $K_{zz}/K = 0.08$, $\eta_K = 0$. Note that the measured value of K_{zz}/K is over three times the magnitude of the direct dipolar contribution and of opposite sign. This indicates a large pseudodipolar contribution to the magnetic hyperfine tensor originating from the unit all of the copper atoms.

A satellite observed by Boyce and Slichter in powdered samples of *Cu*Fe was found to have $\Delta K/K = -1.20 \pm 0.03$. Within experimental uncertainty this corresponds to the value for the third shell obtained here and allows the identification of satellite B as due to third shell nuclei.

A satellite, denoted M, was observed by Boyce and Slichter to have a value for $\Delta K/K$ of 1.85 ± 0.03 in powdered samples. Referring to Table II for field orientations of [001], [111], and [110] a satellite is observed with $\Delta K/K$ of 1.87 ± 0.02, 1.87 ± 0.03, and 1.85 ± 0.03, respectively. This strongly suggests a shell of nuclei with an unobservably small anisotropic field shift is giving rise to satellite M. The intensity of the satellite assigned to the third shell is most accurately measured for a field alignment in the [111] direction.

One can use this assignment to compute the number of nuclei giving rise to satellite M using its observed intensities relative to the third shell satellite for this field orientation. Using the measured intensity of satellite M relative to the satellites assigned to the third shell, one can compute the number of nuclei responsible for the satellite M. The resulting number of nuclei is between seven and nine. The only neighbor shells of less than 12 nuclei from among the first ten are the second, sixth, and eighth shells. Since the isotropic field shift of satellite M is larger than that of the third or any other satellites observed in this study, one can assign it to the second shell of nuclei with reasonable certainty.

B. *Cu*Co

1. *Cu*Co *high-field measurements*

^{63}Cu satellite resonances were studied in a single crystal of *Cu*Co (0.084-at.% Co) for an applied magnetic field of 58 kG aligned along several different crystal axes. We identify a number of satellites as arising from the first shell of nuclei neighboring the Co impurity. We can characterize the magnetic hyperfine tensor completely at these nuclei and find evidence for a large pseudodipolar magnetic coupling. The contact term of the magnetic hyperfine interaction was measured for satellites arising from two additional shells of nuclei. We identify one as the second shell of neighboring nuclei on the basis of relative satellite intensities.

Table I presents the measured ^{63}Cu main resonance peak-to-peak linewidth for magnetic field orientations along the crystal major symmetry axes. Figure 2 presents a portion of the NMR absorption derivative spectrum in the region of the ^{63}Cu main resonance in a *Cu*Co single crystal for three different orientations of the magnetic field with respect to the crystal axes. Shown are a number of satellite resonances which, because of their angle-dependent field shifts and relative intensities, we identify as arising from the same shell of nuclei around the Co impurity—a shell of 12 nuclei located in the 011 and equivalent positions. The measurements were performed at fields in the region of 58 kG and at a temperature of 278 K. Using a 3-sec time constant and a modulation field with a peak-to-peak amplitude of 15 G at a frequency of 700 Hz, the ^{63}Cu main resonance had a signal to noise ratio of 200 to 1. The satellite resonances had intensities between (1–0.1)% of the main resonance intensity.

The field shifts of the satellite resonances shown in Fig. 2 are plotted in Fig. 3 as a function of the angle which the magnetic field makes with the [011] axis when rotated in the (1 –1 0) plane. Low-field

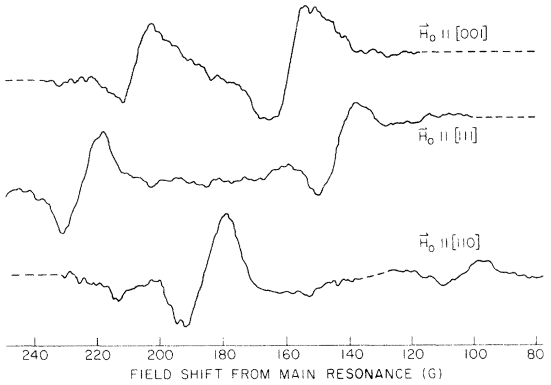

FIG. 2. ^{63}Cu satellite resonance from the first shell of nuclei neighboring the Co atoms in a single crystal of Cu(0.084-at.% Co). The magnetic field is oriented successively along the three major crystal-symmetry axes. The magnetic field is 58 kG, and the temperature is 278 K. A 3-sec lock-in time constant was used and between 100 and 700 sweeps were averaged to produce the spectra shown. Vertical scales are only approximately equal among the traces.

NMR measurements to be described in Sec. IV B 2 demonstrated that these satellites originated from the ^{63}Cu $(\frac{1}{2})$-$(-\frac{1}{2})$ nuclear transition. A small contribution from the quadrupole interaction to the field shifts of these satellites was observed in this low-field study. Since the quadrupole field shifts are inversely proportional to the applied magnetic field strength, at the fields discussed in the present section, such shifts are extrapolated to be on the order of 1% or less of the measured satellite

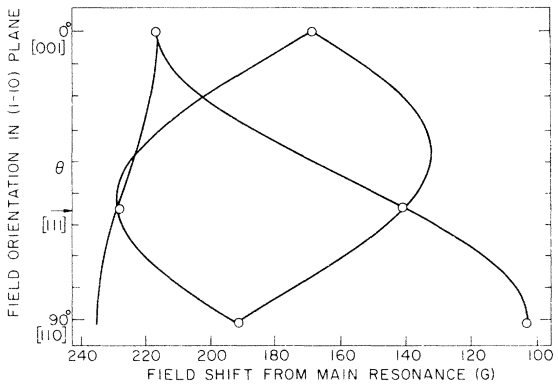

FIG. 3. Field shifts of resonances from the first shell of nuclei neighboring the Co atoms in a single crystal of Cu(0.084-at.% Co) as a function of field orientation in the (1–10) crystal plane. Measurements were made in an external magnetic field of 58 kG and a temperature of 278 K. The width of the circles indicate experimental uncertainty. The curve shown is the total rotation pattern computed for a magnetic hyperfine tensor with a nonzero asymmetry parameter and is described in the text.

field shifts at 58 kG. Nevertheless, the data in Fig. 3 has had these extrapolated quadrupole shifts subtracted.

The solid curve in Fig. 3 was computed using a set of three parameters describing the isotropic and antisotropic field shifts arising from the hyperfine interaction. The nuclei were assumed to lie at the 12 (0, 1, 1) sites around the Co impurity. Referring to the spectra with a [110] field orientation in Fig. 3, the low-intensity satellite of two nuclei expected in the region of 230 G was not conclusively observed due to an uneven baseline and possible satellite broadening. The relative intensities of satellites from nuclei in the first-neighbor shell is shown in Table III.

The (0, 1, 1) symmetry of this shell is unambiguously determined by the rotation pattern of the corresponding satellites. In addition to the first shell, only the fourth, ninth, or some further shells have (0, 1, 1) symmetry and assigning the satellites to any of the latter would imply the unlikely situation that all of the closer shells had nuclei with smaller magnetic hyperfine and electric quadrupole interactions. Therefore, these satellites are assigned to the first shell of nuclei neighboring the Co impurity.

The solid curve in Fig. 3 was fit to the data using the form for the satellite field shifts due to the hyperfine interaction described in Sec. II. The measured value of the contact term is $\Delta K/K = -1.38 \pm 0.01$. The measured values of the magnetic hyperfine tensor components are $(K_{zz}/K)_1 = 0.61 \neq 0.01$ and $\eta_{K1} = 0.23 \pm 0.02$. Adhering to the convention that $|K_{zz}| \geq |K_{yy}| \geq |K_{xx}|$, for a nucleus at the position (0, 1, 1), the principal axes are as follows. X: [100]; Y (Z): [0 1 −1]; Z (Y): [011].

Let us compare the measured value of the hyperfine tensor with a value calculated assuming all of the magnetization associated with the presence of the Co impurity[16] is concentrated in the impurity unit cell and has spherical symmetry. Then, using Eq. (7) and adopting the set of principal axes described above, the calculated values of the components are $K_{zz}/K = 0.20$, $\eta_K = 0$. Another possible source of anisotropic field shifts is due to the spin magnetization in unit cells other than that of the Co impurity and the nucleus being observed. One can obtain an estimate of this change in spin magnetization in a given unit cell by scaling the spin susceptibility per atom of pure copper (1.55×10^{-29} emu-atom) by the measured change in isotropic Knight shift at the nucleus in that cell. Confining the estimate to the first shell of nuclei, the largest component of the hyperfine tensor at a nucleus in the first shell contributed by the spin magnetization in the remaining 11 unit cells in that shell is $K_{zz}/K = 0.0025$ using the above principle axes. This contribution is negligible compared to the measured values. The above estimates indicated that contributions to the measured magnetic hyperfine tensor from outside the unit cell of the first-neighbor copper nucleus being observed accounts for about $\frac{1}{3}$ of the measured value. This implies that a large asymmetric contribution to the anisotropic hyperfine tensor originates in the unit cell of the first-neighbor ^{63}Cu nuclei.

Two additional satellite resonances were observed which showed no variation in their position or shape when the orientation of the external field with respect to the crystal axes was changed. The isotropic field shifts measured for these satellites are $(\Delta K/K)_M = 0.74 \pm 0.01$ and $(\Delta K/K)_B = -0.28 \pm 0.01$, where the satellites have been denoted by the letters B and M, following the scheme of Lo *et al.*[14]

Using the measured intensities of the satellites associated with the first shell of nuclei and the measured intensities of satellites M and B, one can estimate the number of nuclei in their shells of origin. Satellites M and B have intensities relative to the main resonance of 3.6×10^{-3} and 11.0×10^{-3}, respectively. From the first-neighbor intensities listed in Table III, one can conclude that satellite M is due to between 4 and 8 nuclei and satellite B is due to between 12 and 24 nuclei. Satellite M, therefore, arises from either the 2nd, 6th, or 8th shell of nuclei neighboring the Co atom, since these shells contain 6, 8, and 6 nuclei, respectively, and no other shell among the

TABLE III. Relative intensity of first-neighbor satellites in Cu(0.084-at.% Co). Listed are the intensities, expressed as fractions of the ^{63}Cu main resonance intensity, of satellites from the first shell of nuclei neighboring the Co atom in a single crystal of CuCo 0.084 at.%. Intensities were corrected for any observed satellite broadening beyond the main resonance width. Also shown are the number of nuclei in a first-neighbor shell (with a total of 12 nuclei) theoretically attributable to the satellite.

Field orientation	$\Delta K/K$	Fractional intensity	Number of nuclei
[100]	-1.62 ± 0.02	2.0×10^{-3}	4
	-1.26 ± 0.01	3.8×10^{-3}	8
[111]	-1.70 ± 0.02	3.5×10^{-3}	6
	-1.06 ± 0.01	3.1×10^{-3}	6
[110] [a]	-1.43 ± 0.01	3.7×10^{-3}	8
	-0.77 ± 0.01	1.8×10^{-3}	2

[a] An additional satellite from two nuclei is predicted for this field orientation. It was not observed clearly enough to warrant inclusion.

first 10 neighbors contains less than 12 nuclei. Since satellite M has a relatively large field shift, it quite likely originates from the second shell of neighboring nuclei around the Co atom.

The lack of an observable anisotropic shift of the satellite from the second-shell nuclei also implies the existence of contributions from pseudodipolar fields to the anisotropic field shifts when considered along with the first-neighbor measurements. The anisotropic hyperfine coupling at satellite M is less than the minimum observable value of K_{zz}/K, estimate at ± 0.08 and determined primarily by the satellite linewidth. However, if only dipolar coupling caused the first-neighbor anisotropic shifts, then the second neighbor would have the observable value of $K_{zz}/K = 0.21$, since the direct dipolar contribution from the Co unit cell varies simply as $1/r^3$. The pseudodipolar contribution, on the other hand can change sign between nuclei (as the contact term does between the first and second neighbors) and can allow a consistent explanation of the results for the first and second shells.

Results reported here can be compared with other observations of satellite resonances in powdered *Cu*Co alloys by Lang *et al.*[16] The only room-temperature measurement performed in the latter work was made on the satellite corresponding to what was identified here as arising from the first shell of nuclei near the Co impurity. The reported value of $(\Delta K/K)_1$ was -1.56 ± 0.06. In that study, the satellites due to the first-neighbor shell plus the satellites B and M were all observed, however, at 4.2 K and the linear dependence of their field shifts on the external magnetic field strength was verified. A slight temperature dependence to the field shift of the first-neighbor satellite was noted and it is reasonable to assume this reflects the temperature dependence of the impurity susceptibility. One can scale the field shifts measured by Lang *et al.* for the satellites B and M using the ratio of the first-neighbor shifts at 300 K to those at 4.2 K. Their results for then $(\Delta K/K)_M = 0.78 \pm 0.03$ and $(\Delta K/K)_B = 0.30 \pm 0.02$. A smearing of the intensity of the satellite from the first-neighboring shell of nuclei was observed by Lang *et al.* This was interpreted as due to the presence of anisotropic field shifts arising from the direct dipolar coupling with the impurity which were directionally averaged by the powdered samples used. An estimate of K_{zz}/K was made there which is about one-third of the value reported in the present single-crystal experiment, but their estimate was based on an observed powder pattern partially masked by the main resonance.

It has been suggested by Karnezos and Gardner[18] that the satellites observed by Lang *et al.* have the following origin: satellite M is from the third or fourth shell of neighboring nuclei and satellite B is from the second shell. Such identifications would result in a ratio of the intensity of satellite M to that of satellite B of 4 or 2. The corresponding intensity ratio measured in the present single-crystal study of 0.33 clearly rules out such an identification. As indicated above, the measured intensities are consistent with the reverse assignment, in agreement with Lang *et al.*

2. *Cu*Co *low-field measurements*

The satellites identified at 58 kG as due to nuclei in the first shell nearest the Co impurity were observed also at fields between 1.9 and 8.9 kG. The anisotropic field shifts at low fields were found to depend in part on the inverse of the magnetic field strength. Such a field dependence can arise only from the ^{63}Cu $(\frac{1}{2})$-$(-\frac{1}{2})$ transition modified by the second-order quadrupole interaction. These data enable us to determine completely the electric-field-gradient tensor at the first-neighbor site.

The low-field experiments were performed on a single crystal of Cu 0.35-at.% Co at a temperature of 4.2 K. Dependence of the ^{63}Cu main resonance peak-to-peak line width on the magnetic field orientation with respect to the crystal axes at 4.6 kG is shown in Table I. The field shifts of the satellites observed for the magnetic field aligned along the [111] direction are plotted as a function of external field strength in Fig. 4. The broken lines indicate the positions that the two satellites would have if the field shifts were due only to the

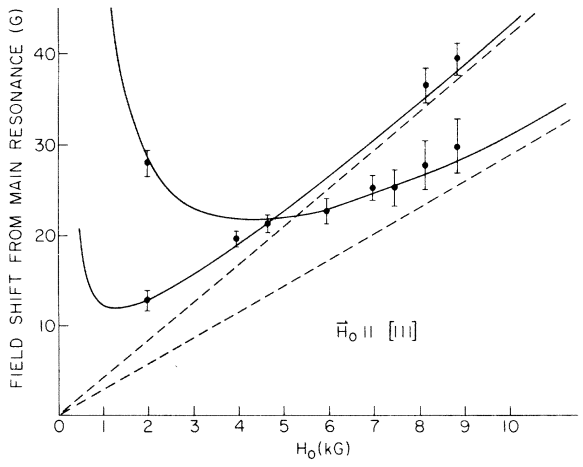

FIG. 4. Satellite field shifts in a Cu(0.35-at.% Co) single crystal as a function of magnetic field strength. The field is aligned along the crystal [111] axis. The broken lines are the magnetic hyperfine field shifts and the solid curves also include the quadrupole shifts deduced from the data.

measured magnetic hyperfine field shifts discussed in Sec. IV B 1. The two satellites observed correspond to the only two satellites (due to six nuclei each) arising from the 12 nuclei in the first shell around the Co impurity for a [111] field orientation.

For a [110] field orientation, a single satellite is observed with an intensity slightly greater than either of the two satellites observed with a [111] field orientation. Figure 5(a) presents the field dependence of this satellite. The broken line is the extrapolated position of the satellite calculated using only the magnetic hyperfine field shift measured at high fields. The satellite is due to the eight nuclei in the first shell of neighbors having the same resonance field for the [110] field orientation. This is known because the observed satellite has a field shift which approaches the calculated shift at high fields and also has the correct intensity relative to the satellites observed for a [111] field orientation.

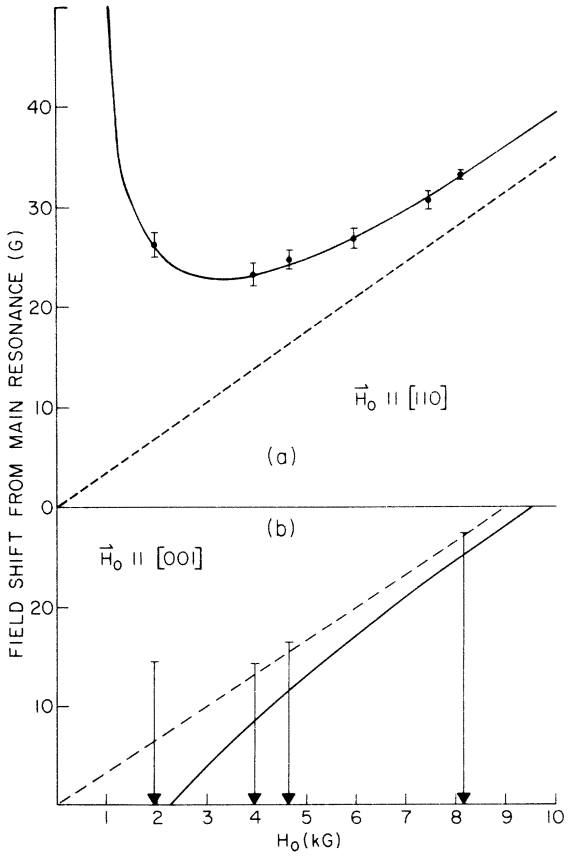

FIG. 5. (a) Satellite field shifts as a function of field strength for a field orientation along the [110] direction in a single crystal of Cu(0.35-at.% Co). (b) Upper limit on satellite field shifts for a satellite obscured by the ^{63}Cu main resonance. The external field is aligned along the crystal [001] direction.

As shown in Fig. 5(b), with the field aligned along the [100] direction, no satellite was resolved. The proximity of the intense ^{63}Cu main resonance renders impossible the observation of satellites which are field shifted less than roughly 10 or 15 G. The broken line in Fig. 5(b) indicates the extrapolated field shifts of the eight nuclei satellite originating from the first-neighbor shell of nuclei and calculated from the measured magnetic hyperfine coupling only.

When the field shifts due to the measured magnetic hyperfine interaction are subtracted from the observed field shifts the remainder exhibits an inverse field dependence characteristic of a field shift due to a second-order electric quadrupole interaction. Note, however, that since the [111] field orientation results in two satellites of equal intensity, there are two possible ways to subtract the two different values of the associated magnetic hyperfine shifts. Nevertheless, only one choice allows the measured field shift, after subtraction of the magnetic shifts, to be explained by a simple field strength dependence, and an inverse field dependence results. This allows the choices of the principal axes of the magnetic hyperfine and EFG tensors to be related, as will be shown below.

The electric-field-gradient tensor at the first shell of nuclei neighboring the Co impurity has been calculated using the field shifts at 2.0 kG after subtraction of the measured magnetic shifts. The EFG parameters which fit the data indicate the [100] directions at the first-neighbor sites are the directions of maximum electric field gradient. The [100] directions are perpendicular to the radius vector joining the Co impurity with the copper nuclei. The principal axes are X (Y): [0 1 −1]; Y (X): [011]; Z: [100]. The alternate choices shown in parenthesis can correspond only to the alternate choices for the magnetic hyperfine tensor of this shell given in Sec. IV B 1. The EFG parameters defined with respect to these principal axes are $\nu_Q = 0.377 \pm 0.014$ MHz and $\eta_Q = 0.50 \pm 0.08$. The solid curves in Figs. 4 and 5 were computed using this EFG tensor as well as the magnetic hyperfine tensor discussed in Sec. IV B 1.

The EFG tensor measured in the present single-crystal study is in disagreement with the EFG tensor components inferred from a spin-echo double-resonance experiment on powdered *Cu*Co alloys by Boyce. Subsequently, it was found that the spin-echo results can be made consistent with the results presented here if the spin-echo data is interpreted in terms of an EFG tensor with the maximum field gradient in the [100] direction for a nucleus at a (0, 1, 1) site, as the present single-crystal work indicates must be the case.

C. *Cu*Ni

^{63}Cu NMR satellite resonances were observed in an alloy single crystal of *Cu*Ni 0.73 at.%. The rotation pattern about the [1−10] axis indicated the satellite resonances originated from the $(\frac{1}{2})$-$(-\frac{1}{2})$ transition, modified predominantly by the quadrupole interaction, of nuclei situated in the [011] directions around a substitutional Ni impurity, corresponding to the first shell of nuclei neighboring the impurity. The electric-field-gradient tensor was completely characterized and a small isotropic shift from the magnetic hyperfine contact term was measured at the first shell of nuclei. Details of these measurements are presented below. A preliminary account of this *Cu*Ni data has been given by us elsewhere[19]; subsequently to that report similar results on *Cu*Ni have been described by Nevald and Petersen.[20]

The measurements were made at 8.1 kG and a temperature of 4.2 K with a peak-to-peak modulation amplitude of 3 G. Owing to the presence of the ^{63}Cu main resonance, satellite resonances with field shifts less than approximately 10–15 G were unobservable. Satellite intensities ranged from 5.5 to 1.5% of the main resonance intensity. Using the shell identification discussed below and the measured impurity concentration, the calculated resonance intensities range from 6.4 to 1.6% of the main resonance intensity. The signals from 10 to 20 field sweeps were averaged. Figure 6 presents a portion of the satellite spectrum for various field orientations. Figure 7 shows the complete rotation pattern with the magnetic field rotated about the crystal [1−10] axes at 10-deg intervals between the [001] and the [110] axes. The solid curve in Fig. 7 was calculated for a set of electric-field-gradient and hyperfine tensor components at the 12 copper nuclei which lie in the [011] directions from the Ni impurity atom. Using the fact that only a shell of copper nuclei with (0, 1, 1) symmetry around a substitute Ni atom could produce the observed rotation pattern together with arguments similar to those used in the case of the *Cu*Co first shell, these satellites are assigned to the first shell of neighboring nuclei. To fit the data, use was made of the positions of the satellite resonances observed when the magnetic field was aligned along the three major crystal symmetry directions since, for these field orientations, no difficulties arose due to satellite resonances incompletely resolved from one another. The field shifts were used to find a theoretical rotation pattern which was the sum of two terms: anisotropic field shifts due to the $(\frac{1}{2})$-$(-\frac{1}{2})$ transition modified

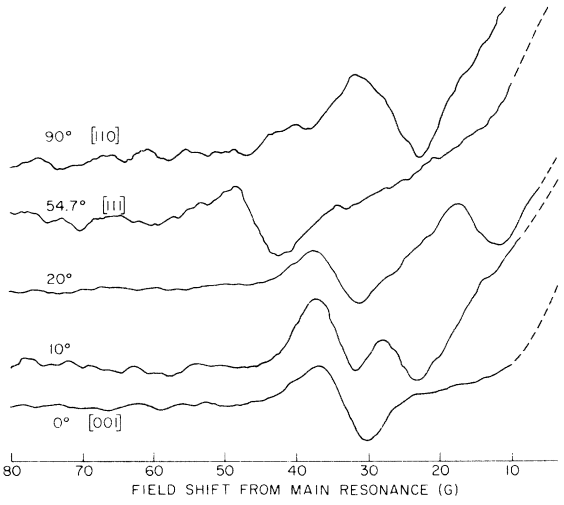

FIG. 6. NMR spectra near the ^{63}Cu main resonance in a single crystal of Cu(0.73-at.% Ni) for various orientations of the static magnetic field in the crystal (1 − 10) plane. The measurements were made at 8.1 kG and a temperature of 4.2 K. A lock-in time constant of 3 sec and a modulation peak-to-peak amplitude of 3 G at 150 Hz were used. The traces shown are the result of 20 averaged sweeps. Vertical scales are only approximately equal.

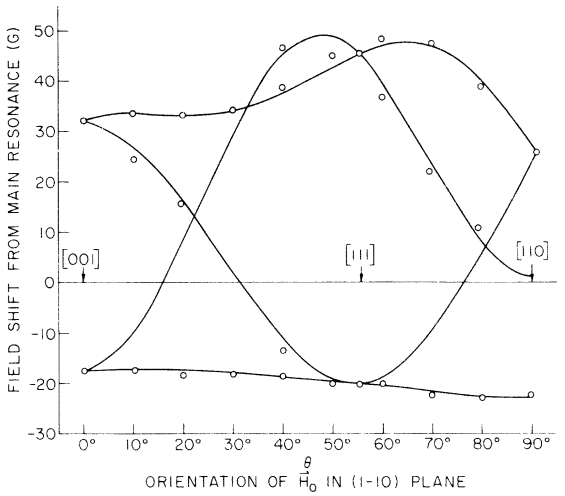

FIG. 7. Complete angular dependence of the ^{63}Cu satellite resonance field shifts in a single crystal Cu(0.73-at.% Ni) the static magnetic field is rotated in the (1−10) plane. θ is the angle between the magnetic field and the [011] direction. The measurements were made at 8.1 kG and 4.2 K. All of the resonances originate from the first shell of nuclei neighboring the Ni impurity. The nuclear quadrupole interaction due to local electric field gradients is responsible for the large anisotropy of the field shifts. The EFG and hyperfine tensor components with which the solid curve was computed are described in Sec. IV C. The absence of observed satellite field shifts between roughly −12 and +12 G is due to the presence of the main resonance which has about 50 times the satellite intensities.

by the quadrupole interaction plus a small isotropic field shift due to the contact term of the magnetic hyperfine interaction. The quadrupole interaction clearly dominates the satellite field shifts. The EFG parameters determined here were $\nu_Q = 1.12 \pm 0.02$ MHz, $\eta_Q = 0.21 \pm 0.03$ defined with respect to the following principal axes for a nucleus in a (0, 1, 1) position. X (Z): [0 −1 1]; Y: [100]; Z (X): [011].

The magnetic isotropic field shift is quite small, but definitely positive: 2.0 ± 0.7 G in an external magnetic field of 8.1 kG. The corresponding normalized change in Knight shift due to the contact hyperfine interaction is $\Delta K/K = -0.11 \pm 0.04$.

Values obtained for ν_Q, η_Q, and $\Delta K/K$ in other experiments using powdered CuNi samples[14] are in agreement with the values obtained here. In experiments with powdered samples, no direct information can be obtained concerning the symmetry of the nuclei being observed or the principal axes of the EFG tensor. Lo *et al.* concluded that $\nu_Q = 1.1 \pm 0.1$ MHz, $\eta_Q = 0.20 \pm 0.05$, and $\Delta K/K = -0.11 \pm 0.02$ in steady-state NMR studies performed on powdered samples at fields up to 60 kG. A zero-field double-resonance experiment on powdered CuNi reported by Whalley and Slichter[21] determined the quantity $\nu_Q(1 + \frac{1}{3}\eta_Q^2)^{1/2}$ for four shells of nuclei. The largest value of this quantity measured was 1.125 MHz. Using the EFG parameters found in the present work, one arrives at the corresponding value of 1.13 ± 0.02 MHz. Of the three remaining shells observed in the zero-field study, the largest value of $\nu_Q(1 + \frac{1}{3}\eta_Q^2)^{1/2}$ was 0.224 MHz. Even though the second-order quadrupole satellite field shifts are inversely proportional to the applied field, satellites corresponding to the latter quantity would lie well beneath the main resonance at 1.8 kG, the lowest field used in this study.

V. IDENTIFICATION OF SATELLITE SHELLS

The most direct use of the above data is to deduce the shell of nuclei neighboring the impurity atom from which the satellite resources originate. In summary, when single rotation crystal patterns of the satellite field shifts were compared with the corresponding theoretical predictions based on the crystal symmetry of the shells of copper, nuclei neighboring the impurity satellites from the following shells were identified CuNi, first; CuCo, first and second; CuFe, second and third.

The Friedel-Anderson virtual bound-state model of a magnetic impurity leads to a calculation of phase shifts for the up-spin and down-spin conduction-electron wave functions, hence to an integral over the conduction band which gives the spin density at nearby nuclear sites. In principle, one can thus use the measured ΔK's to deduce the positions and widths of the d-wave resonances. This process is complicated by the fact that the parameters occur in an integral so that each trial value of parameters requires a numerical integration. Jena and Geldart, however, have developed approximate expressions which give algebraic relationships between the spin density and the level parameters. Using these relations, Boyce and Slichter[5] have determined the positions and widths of the d-wave resonances using our identification of satellites. They found it necessary to include crystal-field splitting of the iron d-orbital levels as suggested by the asymmetric hyperfine field tensors discussed below. T. Aton is conducting experiments on Mn- and Cr-doped copper single crystals to identify satellite resonances observed in the respective powdered samples with a view to deducing the levels and widths in those cases.

VI. MAGNETIC HYPERFINE AND ELECTRIC QUADRUPOLE COUPLING

A. Origin

We discuss the origin of the traceless magnetic hyperfine and electric quadrupole tensors which give rise to the anisotropic field satellite shifts measured above.

Consider first the simplest possible picutre of the host plus magnetic impurity. Take the copper host to be of uniform "jellium." Consider the magnetic impurity to be a spherically symmetric resonant potential described by the Friedel-Anderson model and that we observe a Cu nucleus located in the jellium at a normal lattice position. As is well known, spherically symmetric oscillations are set up in the conduction-electron charge and spin density near the impurity. This leads to a nonvanishing K_{zz} and V_{zz} in Eqs. (6) and (10), respectively, where z is the axis from the impurity to the nucleus in question. (These equations suggest that the pseudodipolar and quadrupolar couplings may be related. This is discussed below.) However, thus far, the variation in charge and spin density must be independent of direction in any plane normal to a radius vector from the impurity. That is to say, the coupling tensors are symmetric: η_K and η_Q are zero.

Next, allow the host nuclei to appear as a perfect rigid lattice of scattering potentials. Direct electric scattering from a spherically symmetric potential plus a cubic lattice cannot result in asymmetric spin distributions at a near-neighbor site. Experiments with nonmagnetic impurities dissolved in copper indicate that the relaxation of the host lattice around the impurity may be responsible for

the EFG asymmetry at near-neighbor nuclei. However, scattering from the noncubic potential arising from the relaxed lattice is spin independent and cannot cause asymmetry in the magnetic hyperfine coupling.

On the other hand, asymmetry in the magnetic coupling can arise due to scattering from the nonspherical potential resulting from crystal-field splitting of the impurity d-orbital virtual bound states. The asymmetry of the magnetic hyperfine coupling at near neighbors to a magnetic impurity may therefore be a probe of impurity state crystal-field splitting.

An additional contribution originates in the anisotropic momentum surfaces of constant energy which is evidenced by the anisotropic Fermi surface of copper. The latter contribution should be more important at host nuclei removed from the impurity by more than a distance of $1/\Delta k_F = 5.6$ Å, where Δk_F is the variation in k_F over the Fermi surface. This is nearly the fifth-neighbor distance in copper.

B. Relation of pseudodipolar to quadrupolar coupling

The existence of a scattering resonance will produce phase shifts and thus change the conduction-electron wave function in the vicinity of an impurity from its value in the absence of the impurity. Since the pure metal has cubic symmetry, a nucleus experiences no electric field gradients, but the existence of the phase shifts when an impurity is present gives rise to a conduction-electron contribution to the electric field gradient. If the impurity has a net spin, the energies at which the up-spin and down-spin resonances occur differ, giving rise to a spin oscillation with concomitant isotropic Knight shift and pseudodipolar coupling. In this section we show that there is a relationship between the two. This calculation corrects an earlier incorrect one inflicted by Slichter on his coworkers Lang, Lo, and Boyce.[16]

For a single electron with spin $m = +\frac{1}{2}$ quantizied along the z direction, there is a contribution to the electric field gradient V_{zz} and the corresponding frequency ν_{zz}

$$\nu_{zz}^i = eQV_{zz}^e/4\pi h = \frac{3e^2Q}{2I(2I-1)h}\langle\psi_i|\frac{3\cos^2\theta_i - 1}{r_i^3}|\psi_i\rangle, \quad (15)$$

where the subscript i labels the ith electron located at (r, θ, ϕ) in spherical coordinates, with θ the angle between $\vec{r}$ and the z axis, and ψ_i is the wave function of the electron. This holds true whether or not z is a principal axis of the field gradient.

Likewise, this electron contributes a pseudodipolar field H_{pd}, in the z direction of

$$H_{pd}(i) = -\gamma_e \hbar m_i \langle\psi_i|(3\cos^2\theta - 1)/r_i^3|\psi_i\rangle. \quad (16)$$

If the external static field H_0 is in the z direction, this pseudodipolar field will shift the nuclear resonance of a nucleus at $r = 0$ by $H_{pd}^z(i)$ in units of magnetic field. This is true whether or not the z axis is a principal axis of the Knight-shift tensor provided H_0 is much bigger than the pseudodipolar fields.

We now apply these ideas to an atom which is magnetic in the Anderson sense. Referring to Fig. 8 we see, the two configurations A and B with scattering resonance for up spins and down spins. Let the probability of occurrence of the states be p_A and p_B. They differ from each another when there is a net magnetization of the magnetic atom, as when H_0 is applied. Calling the z component of magnetization of configuration A, μ_{zA}, we have

$$\mu_{zA} = -\mu_{zB} \quad (17)$$

and the thermal average of M_z, $\langle M_z\rangle$, is

$$\langle\mu\rangle = \mu_{zA}p_A + \mu_{zB}p_B = \mu_{zA}(p_A - p_B) = \chi H_0. \quad (18)$$

Thus

$$p_A - p_B = \chi H_0/\mu_{zA}, \quad (19)$$

$$p_A - p_B = \chi H_0/\gamma_e\hbar S, \quad (20)$$

where S is the "net spin" of the magnetic atom. Consider the state A. The down spins contribute to ν_Q and amount we denote by $\nu_Q(A, -)$ of

$$\nu_{zz}(A, -) = \frac{3e^2Q}{2I(2I-1)h}\sum_{A,-}\langle\psi_i|\frac{3\cos^2\theta - 1}{r^3}|\psi_i\rangle, \quad (21)$$

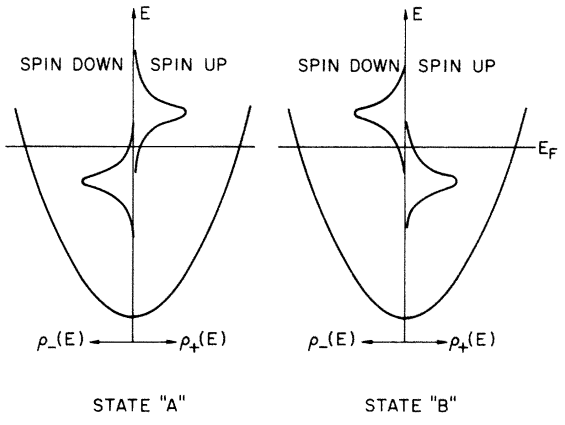

FIG. 8. Density of states in the Anderson model, showing the densities $\rho_+(E)$ and $\rho_-(E)$ of up- and down-spin electrons vs energy E. The parabolic curves of a free electron are shown as are the extra Lorentzian densities contributed by the magnetic impurity.

where $\sum_{A,-}$ denotes a sum over states, i, which are down-spin states of A. Or, evaluating numerically,

$$\nu_{zz}(A,-) = 2.79\times 10^{-18} \sum_{A,-} \langle \psi_i | \frac{3\cos^2\theta - 1}{r^3} | \psi_i \rangle . \tag{22}$$

In general, then

$$H_{pd}(A,m) = -(\gamma\hbar m)\nu_{zz}(A,m)/(2.79\times 10^{-18}). \tag{23}$$

Thus

$$H_{pd} = \sum_m [p_A H_{pd}(A,m) + p_B H_{pd}(B,m)] . \tag{24}$$

Now

$$H_{pd}(A,m) = -H_{pd}(B,-m). \tag{25}$$

Thus we get

$$H_{pd} = \sum_m (p_A - p_B) H_{pd}(A,m), \tag{26}$$

which, using Eqs. (23) and (25) gives

$$H_{pd} = \frac{\chi H_0}{S}\frac{1}{2}\frac{\nu_{zz}(A,-) - \nu_{zz}(A,+)}{2.79\times 10^{-18}}. \tag{27}$$

Note this equation relates the component of pseudodipolar field along the direction of H_0 (the z direction) with the contributions of the d-wave electrons to the electric field gradient V_{zz} and corresponding frequency ν_{zz}. Note that the z direction does not need to be a principal axis of the quadrupole coupling *or* of the pseudodipolar coupling.

Consider Fe, with $\chi = 7.28\times 10^{-27}$ and $S = 1.25$. Take $\nu_{zz}(A,-) - \nu_{zz}(A,+) = 10^6$ Hz as typical of a first neighbor, and $H_0 = 60$ kG. Then

$$H_{pd} = 63 \text{ G}, \tag{28}$$

compared with a value of the direct dipolar field at a first-neighbor site which ranges from 52 to -26 G.

Since we find that in general the pseudodipolar coupling is comparable in magnitude to the direct, we see that we can conclude that the d-wave resonances contribute quadrupole couplings of order 1 Mhz at the first-neighbor position, and are thus major contributors to the observed field gradients.

Our estimate above applied to atoms which are magnetic in the Anderson sense — i.e., the up-spin and down-spin resonances occur at different energies. For an atom which is nonmagnetic in Anderson's sense, the up- and down-spin resonances coincide in the absence of an applied field. Application of an applied field causes the up-spin and down-spin conduction bands to displace in energy, with a resultant repopulation of the d-wave resonances. The resultant pseudodipolar field H_{pd} then becomes

$$H_{pd} = f[\tfrac{1}{2}\gamma\hbar/(2.79\times 10^{-18})]\nu_{zz}, \tag{29}$$

where f is a ratio of the number of electrons whose population shifts, on application of the static field, to the total number of electrons giving rise to the quadrupolar coupling. A good approximation is

$$f = \gamma\hbar H_0/\Delta E = 7\times 10^{-4} \tag{30}$$

for $H_0 = 6$ kG and $\Delta E = 1$ eV. For the measured ν_{zz} at the nearest neighbor of a Co impurity, this gives $H_{pd} \simeq 0.17$ G, negligible compared to the 57-G pseudodipolar field. A similar contribution arises for an atom which is magnetic in the Anderson sense, since there is also a similar repopulation effect there.

Referring to the same set of principal axes with a z-axis radial from the cobalt impurity and subtracting the direction dipolar part of K_{zz}, the measured asymmetry parameters are $\eta_K = 0.32$ and $\eta_Q = 1.67$.

This difference can reflect several things, including the minus sign in Eq. (27) and the fact that whereas the measured pseudodipolar couplings can originate only from d-wave scattering by the magnetic impurity, substantial contributions to the EFG can come also s and p wave scattering and lattice distortion near the impurity.

C. Quadrupole coupling of Ni and Co nearest neighbors

NMR measurements by a number of workers have given the quadrupole couplings at the nearest neighbors to many nonmagnetic impurities in copper. There has been no successful theoretical description of these results. Schumacher pointed out that the measured quadrupole asymmetry parameter of the first neighbor is roughly proportional to the valence difference of the nonmagnetic impurity and copper. Nevald has improved this empirical rule by comparing the effective valence difference corrected for lattice relaxation against the measured difference $|V_{xx} - - V_{yy}|$. Using the proportionality constant so obtained of 0.22 Å^{-3}/(electronic charge) and the first-neighbor quadrupole couplings measured here for Co and Ni nearest neighbors, the necessary valence difference to continue this trend into the $3d$ element impurities can be calculated. One finds -0.84 (± -0.09) electrons for Ni. These values are strikingly low when compared with the total valence difference of -2 and -1 between Co and Ni, respectively, and copper. We note also the small values of ν_q measured for Ni and especially Co nearest neighbors relative to that for non-$3d$ impurities.

APPENDIX A: THEOREM ON THE AVERAGE MAGNETIC HYPERFINE FIELD SHIFT OF A SHELL OF NUCLEI

In this appendix we prove a theorem which is useful in identifying which satellite lines in a single crystal go with a given satellite seen in a powder pattern. The theorem states that the center of gravity of a single-crystal spectrum coincides with that of a powder spectrum for any orientation of the applied field relative to the crystal axes.

Consider a static magnetic field $\vec{H}_0$ applied in an arbitrary direction with respect to the crystal axes of an alloy single crystal. Suppose the field shifts of the satellites from a certain shell of nuclei around a magnetic impurity are due only to the magnetic hyperfine interaction. Form the sum of the field shifts δH_i of each nucleus in the shell and divide by the number of nuclei in the shell N. The result, which is by definition the center of gravity of the spectrum, is equal to the isotropic field shift $-H_0\Delta K$ for that shell and therefore independent of field orientation:

$$\frac{1}{N}\sum_{i}^{N}\delta H_i = -H_0\Delta K. \tag{A1}$$

To prove this it is sufficient to show that the anisotropic hyperfine field shift averaged over all nuclei in a shell is zero, no matter what the orientation of $\vec{H}_0$. For a single nucleus, the anisotropic shift δH_i^a is

$$\delta H^a(\theta_i,\phi_i) = -H_0K[Y_{2,0}+\eta_K(Y_{2,2}+Y_{2,-2})/\sqrt{2}\,], \tag{A2}$$

where (θ_i,ϕ_i) are the spherical coordinates of the magnetic field $\vec{P}_0$ in the principal-axes system of the hyperfine tensor of the ith nucleus and the $Y_{lm}(\theta,\phi)$ are the spherical harmonics.

Now the fact that the crystal has cubic symmetry means that there are a set of separate and distinct symmetry operations which transform the crystal into itself, leaving the magnetic atom alone, but changing the position in space of the N atoms in a shell. There are 48 such operations for the cubic symmetry (O_h) of the site. If we define $\langle\delta H_i^a\rangle$ as the average of δH_i^a over all 48 operations, clearly

$$\frac{1}{N}\sum_{i=1}^{N}\delta H_i^a = \frac{1}{N}\sum_{i=1}^{N}\langle\delta H_i^a\rangle, \tag{A3a}$$

$$\frac{1}{N}\sum_{i=1}^{N}\delta H_i^a = \langle\delta H_i^a\rangle, \tag{A3b}$$

where in the last line we have made use of the fact that $\langle\delta H_i^a\rangle$ is independent of i.

We can as well view the problem another way. Instead of holding the magnetic field fixed and transforming the crystal orientation, we can hold the crystal fixed and apply the inverse transformations to the field. We then consider the average coupling of one nucleus with a magnetic field pointing along the 48 directions $\hat{r}_s$ produced by the inverse transformations. Thus we have

$$\langle\delta H_i^a\rangle = \frac{1}{48}\sum_{\hat{r}_s}\int \delta H_i^a(\theta,\phi)\,\delta(\hat{r}-\hat{r}_s)\,d\hat{r}. \tag{A4}$$

It is useful to define the function $f(\hat{r})$ as

$$f(\hat{r}) = \frac{1}{48}\sum_{r_s}\delta(\hat{r}-\hat{r}_s), \tag{A5}$$

giving

$$\frac{1}{N}\sum_{i=1}^{N}\delta H_i^a = \int \delta H_i^a\, f(\hat{r})\,dr. \tag{A6}$$

The means of generating the 48 vectors $\hat{r}_s$ shows that they are distributed in angle such that their tips on a unit sphere are distributed with cubic symmetry. Thus, we can expand $f(\hat{r})$ in spherical harmonics of cubic symmetry. Only $l=0$, 4, and higher are used. In terms of a set of cubic axes, we can then reexpress $\delta H_i^a(\theta,\phi)$, giving

$$\frac{1}{N}\sum_{i=1}^{N}\delta H_i^a = \sum_{m=-2}^{+2}\alpha_m\int Y_{2m}(\hat{r})f(\hat{r})\,d\hat{r}. \tag{A7}$$

Expressing $f(\hat{r})$ then in spherical harmonics we see that the right-hand side of Eq. (A7) vanishes, thus proving our theorem that the average anisotropic splitting vanishes.

---

*Present address: Dept. of Physics, Ohio State University, Columbus, Ohio 43210.

[1]J. Kondo, in *Solid State Physics*, edited by F. Seitz, D. Turnbull, and H. Ehrenreich (Academic, New York, 1969), Vol. 23.

[2]A. J. Heeger, in *Solid State Physics*, edited by F. Seitz, D. Turnbull, and H. Ehrenreich (Academic, New York, 1969), Vol. 23.

[3]A. Narath, CRC Crit. Rev. Solid State Sci. 3, 1 (1972).

[4]J. B. Boyce, T. J. Aton, and C. P. Slichter, AIP Conf. Proc. 18, 252 (1974); C. P. Slichter, *ibid.* 29, 306 (1976).

[5]J. B. Boyce and C. P. Slichter, Phys. Rev. B 13, 379 (1976). This paper contains references to many experimental papers concerning satellites.

[6]R. T. Schumacher and George Schnakenberg, Jr., Solid State Commun. 7, 1735 (1969).

[7]George Schnakenberg, Jr., and R. T. Schumacher, Phys. Rev. B 7, 2292 (1973).

[8]B. L. Jensen, R. Nevald, and D. L. Williams, J. Phys. F 2, 169 (1972).

[9]P. W. Anderson, Phys. Rev. 124, 41 (1961).

[10]See, for example, (a) C. P. Slichter, *Principles of Magnetic Resonance* (Harper and Row, New York, 1963); (b) R. E. Walstedt and Y. Yafet, Solid State Commun. 15, 1855 (1974).
[11]M. H. Cohen and F. Reif, in *Solid State Physics*, edited by F. Seitz and D. Turnbull (Academic, New York, 1957), Vol. 5.
[12]W. Kohn and S. H. Vosko, Phys. Rev. 119, 912 (1960).
[13]K. Nanta, J. Umeda, and H. Kusumoto, J. Chem. Phys. 44, 2719 (1966).
[14]D. C. Lo, D. V. Lang, J. B. Boyce, and C. P. Slichter, Phys. Rev. B 8, 973 (1973).
[15]F. W. Young, Jr., and J. R. Savage, J. Appl. Phys. 35, 1917 (1964).
[16]D. V. Lang, J. B. Boyce, D. C. Lo, and C. P. Slichter, Phys. Rev. Lett. 29, 776 (1972); D. V. Lang, D. C. Lo, J. B. Boyce, and C. P. Slichter, Phys. Rev. B 9, 3077 (1974).
[17]P. L. Sagalyn and J. A. Hofmann, Phys. Rev. 127, 68 (1962).
[18]N. Karnezos and J. A. Gardner, Phys. Rev. B 9, 3106 (1974).
[19]T. S. Stakelon and C. P. Slichter, Bull. Am. Phys. Soc. 20, 320 (1975).
[20]R. Nevald and G. Petersen, J. Phys. F 5, 1778 (1975); R. Nevald, *ibid.* 5, L181 (1975).
[21]L. R. Walley and C. P. Slichter, Phys. Rev. B 9, 3793 (1974).